

# UC Davis

## UC Davis Previously Published Works

### Title

Comprehensive Clinical, Diagnostic, and Advanced Imaging Characterization of the Ocular Surface in Spontaneous Aqueous Deficient Dry Eye Disease in Dogs.

### Permalink

<https://escholarship.org/uc/item/0244p3pq>

### Journal

Cornea, 38(12)

### ISSN

0277-3740

### Authors

Leonard, Brian C  
Stewart, Kathleen A  
Shaw, Gillian C  
[et al.](#)

### Publication Date

2019-12-01

### DOI

10.1097/ico.0000000000002081

Peer reviewed



Published in final edited form as:

*Cornea*. 2019 December ; 38(12): 1568–1575. doi:10.1097/ICO.0000000000002081.

## Comprehensive Clinical, Diagnostic, and Advanced Imaging Characterization of the Ocular Surface in Spontaneous Aqueous Deficient Dry Eye Disease in Dogs

Brian C. Leonard, DVM, PhD<sup>\*</sup>, Kathleen A. Stewart, DVM<sup>\*</sup>, Gillian C. Shaw, DVM, MS, PhD<sup>†</sup>, Alyssa L. Hoehn, BS<sup>\*</sup>, Amelia A. Stanley, BA<sup>\*</sup>, Christopher J. Murphy, DVM, PhD<sup>\*,‡</sup>, Sara M. Thomasy, DVM, PhD<sup>\*,‡</sup>

<sup>\*</sup> Department of Surgical and Radiological Sciences, School of Veterinary Medicine, University of California, Davis, Davis, CA

<sup>†</sup> Comparative Ocular Pathology Laboratory of Wisconsin, University of Wisconsin- Madison, Madison, WI

<sup>‡</sup> Department of Ophthalmology & Vision Science, School of Medicine, University of California, Davis, Davis, CA.

### Abstract

**Purpose**—To perform a comprehensive clinical, diagnostic, and imaging characterization of the ocular surface in West Highland White Terriers (WHWTs) diagnosed with aqueous deficient dry eye (ADDE) disease.

**Methods**—Six ADDE-affected and 13 ADDE-unaffected WHWT dogs were enrolled and underwent clinical assessment and disease scoring, tear osmolarity, phenol red thread test, Schirmer tear test, tear film breakup time, fluorescein staining, Rose bengal and lissamine green vital dye staining, meibometry, corneal esthesiometry, ultrasound pachymetry, optical coherence tomography, in vivo confocal microscopy, and conjunctival biopsy. Subjective assessment of their condition was provided by owner-reported surveys.

**Results**—ADDE-affected WHWT dogs had higher median clinical disease (conjunctiva: 5.75 vs. 0.00; cornea: 14.00 vs. 5.00; total: 17.50 vs. 5.00), vital staining (Rose bengal: 2.25 vs. 1.50; lissamine green: 2.00 vs. 1.00), and histologic disease (conjunctiva: 2 vs. 0) scores when compared with the controls. In addition, ADDE-affected WHWTs had significantly lower phenol red thread test (5.0 vs. 17.5, mm/15 s), Schirmer tear test (3 vs. 20, mm/min), tear film breakup time (3.6 vs. 13.9, s) values and higher area under the curve values for meibometry (394 vs. 245, meibometry units [MU]). There were no significant differences in other tear film tests performed. Advanced imaging revealed decreased tear meniscus height (optical coherence tomography) and variable pigment deposition within corneal epithelial cells (in vivo confocal microscopy).

Correspondence: Sara M. Thomasy, DVM, PhD, Department of Surgical and Radiological Science, School of Veterinary Medicine, 1 Shields Avenue, University of California, Davis, CA 95616 (smthomasy@ucdavis.edu).

The authors have no conflicts of interest to disclose.

Supplemental digital content is available for this article. Direct URL citations appear in the printed text and are provided in the HTML and PDF versions of this article on the journal's Web site ([www.corneajrnl.com](http://www.corneajrnl.com)).

**Conclusions**—This comprehensive assessment of ADDE-affected WHWTs depicts the ocular surface changes associated with quantitative lacrimal gland dysfunction. Importantly, ADDE-affected WHWTs may prove a valuable naturally occurring ADDE model for investigating underlying pathophysiological mechanisms and the development of novel therapeutics.

### Keywords

dry eye disease; keratoconjunctivitis sicca; West Highland White Terrier; dog

---

Dry eye disease (DED) represents a multifactorial disorder that is characterized by the instability of the tear film, leading to ocular surface inflammation, irritation, and compromise of vision.<sup>1</sup> Because of the high prevalence of DED, it has a substantial economic impact in the United States with approximately 3.84 billion dollars expended within the US health care system.<sup>2</sup> Human patients with DED can be subcategorized into 2 large groups, 1) aqueous deficient dry eye (ADDE) and 2) evaporative dry eye, with evaporative dry eye being more common.<sup>3</sup> There are only 2 food and drug administration (FDA)-approved medications for treating DED, immunomodulatory medications cyclosporine and lifitegrast.<sup>4,5</sup> Both of these therapeutics had proof of concept established in canine veterinary patients with spontaneous ADDE before being approved for treatment of DED in human patients.<sup>6,7</sup> Despite significant therapeutic improvement in subsets of patients with DED, not all patients have amelioration of their clinical signs and symptoms.<sup>8</sup> The provision of additional models of DED, including naturally occurring disease that is observed in the companion animal population, holds promise for identification and development of novel therapeutics for the treatment of DEDs in human and veterinary patients.

There are multiple causes of ADDE in dogs including metabolic disease, neurologic deficiency, drug toxicity, and surgical excision of lacrimal tissue.<sup>9</sup> However, the most common cause of ADDE in dogs is an insidious immune-mediated compromise of lacrimal gland function, analogous to human patients with Sjögren syndrome, although a salivary component is only rarely observed in dogs and no systemic manifestation of autoimmune disease has been reported in dogs to date.<sup>10,11</sup> Clinical signs can vary in severity but typically include blepharospasm, tenacious mucoid to mucopurulent discharge, erythema of the eyelids, hyperemia of the conjunctiva, and scarring of the cornea.<sup>9</sup> The diagnosis of ADDE is based on this constellation of clinical signs and a Schirmer tear test (STT) result of 14 mm or less after 1 minute.<sup>9</sup> Importantly, there are breeds that are predisposed to the development of ADDE, including the West Highland White Terrier (WHWT) breed having a high relative risk when compared with other breeds.<sup>12</sup> Because of the suspected heritability of ADDE in the breed, WHWTs are good candidates for studying genetic abnormalities that lead to ADDE development, while also serving as a potential model for better understanding underlying pathophysiological mechanisms and facilitating development of novel DED therapeutics.<sup>7,13,14</sup>

The most recent Dry Eye Workshop report detailed many of the diagnostic criteria and tests that aid in the identification of human patients with DED.<sup>15</sup> Widely used diagnostic tests include traditional tear quality and composition assays, such as tear film breakup time

(TFBUT) and tear osmolarity, with newer advanced imaging modalities [eg, optical coherence tomography (OCT) and in vivo confocal microscopy (IVCM)] also being used to evaluate the tear meniscus and alterations to the corneal epithelium and anterior stroma.<sup>15</sup> Given the range of signs and symptoms for DEDs, clinicians typically use multiple diagnostic tests to more accurately diagnose DED and formulate treatment strategies.<sup>15</sup> Assembling data from multiple end points also allows for more broad comparability of patient data between studies and clinicians, allowing further subcategorization of patients into groups and initiation of the most efficacious treatment plan.

The goal of this study was to perform a comprehensive clinical, diagnostic, and advanced imaging assessment of the tear film and ocular surface in WHWT dogs affected with ADDE. We hypothesized that ADDE-affected animals would have clinical scoring and tear film diagnostic values consistent with an aqueous tear deficient disease. In addition, we hypothesized that advanced imaging modalities, such as OCT and IVCM, would enhance characterization of the pathology of the ocular surface (eg, neovascularization, pigmentation, fibrosis) and tear film dynamics in WHWTs with ADDE.

## MATERIALS AND METHODS

### Study Population and Design

This study was approved by the Institutional Animal Care and Use Committee of the University of California, Davis (#18024), and performed according to the Association for Research in Vision and Ophthalmology resolution on the use of animals in research. For affected dogs, inclusion criteria were WHWTs with bilateral clinical signs of ADDE (mucoïd to mucopurulent discharge, conjunctival hyperemia/chemosis, evidence chronic keratitis) and a STT value <15 mm/min.<sup>12</sup> For control dogs, inclusion criteria were WHWTs with no history or clinical signs of ocular disease oculus uterque (OU). Exclusion criteria for both groups were diagnosis of a systemic disease that could affect tear production including diabetes mellitus, hyperadrenocorticism or hypothyroidism, or recent and/or chronic use of oral drugs such as sulfonamides or etodolac, which have been associated with the development of ADDE or the presence of corneal ulceration.<sup>14,16-19</sup> Affected dogs stopped their current medication regimen less than or equal to 1 week prior to initial ophthalmic examination. Additional diagnostics and imaging were performed on a later date, therefore ADDE-affected dogs were treated with artificial tear ointment (Rugby Laboratories, Livonia, MI) until the morning of these tests, in an effort to provide comfort between dates yet not influence testing results. All tests were performed in the order listed to minimize interference between tests; at least 10 minutes lapsed between some tests to permit the ocular surface to recover.<sup>20,21</sup> All tests were conducted in the right eye, followed by the left eye unless otherwise specified.

### Tear and Ocular Surface Diagnostics

Tear film osmolarity (mOsm/L) was measured by electrical impedance (TearLab Osmolarity System; TearLab Corp, San Diego, CA). Samples were collected by placing the test card in the inferior tear meniscus adjacent to the temporal canthus. Aqueous tear production was assessed using the phenol red thread test (PRTT) (Zone-Quick Phenol Red Thread; Showa

Yakuhin Kako Co Ltd, Tokyo, Japan) and STT-I (Intervet Inc, Summit, NJ) for 15 seconds or 60 seconds, respectively, and measured at least 10 minutes apart.<sup>22</sup> The lipid tear component was measured using a Meibometer MB 560 (Courage + Khazaka electronic GmbH, Cologne, Germany). The meibometer tape loop was held for 2 seconds at the inferior eyelid and subsequently analyzed as previously detailed.<sup>21</sup> Results were recorded as mean peak values and mean area under the curve (area under the curve, in arbitrary meibometer units [MU]) from 3 repeated measures of the tape. A Luneau Cochet–Bonnet esthesiometer (12/100 mm; Luneau Ophtalmologie, Prunay-le-Gillon, France) was used to determine the sensitivity of the cornea. The microfilament was extended (6 cm) and incrementally shortened until the patient displayed a blink reflex in response to at least 3 of 5 stimulations. The length of the microfilament was converted to a corneal touch threshold with values of pressure in g/mm<sup>2</sup> using the conversion chart.

### **Slit-Lamp Biomicroscopy and Anterior Segment Scoring and Photography**

Slit-lamp biomicroscopy (SL-15; Kowa American Corporation, Torrance, CA) was performed by a board-certified veterinary ophthalmologist (S.M.T.) and scored using Supplemental Digital Content 1 (see Appendix 1, <http://links.lww.com/ICO/A873>). Imaging was performed with a digital single-lens reflex camera (Canon ROS 5D; Canon Inc, Tokyo, Japan) at an aperture of *f*/18 or *f*/22 (Canon Macro Lens EF 100 mm 1:2:8) and flash setting at 1/4 (Canon Macro Twin Lite MT-24EX 58 mm).

### **Tear Film Breakup Time and Ocular Surface Staining**

TFBUT was determined using a 1% fluorescein solution (OcuSOFT Eyewash Altaire Pharmaceuticals, Inc, Aquebogue, NY; 10% fluorescein solution; Millipore-Sigma, St. Louis, MO) and by measuring the time from manual eyelid opening to the first signs of tear film breakup. The integrity of the epithelium was then assessed and scored (see Appendix 1, Supplemental Digital Content 1, <http://links.lww.com/ICO/A873>). In addition, vital stains Rose bengal (GloStrips Rose Bengal Ophthalmic Strips USP; Amcon Laboratories, Inc, St. Louis, MO) and lissamine green (Green Glo Lissamine Green Ophthalmic Strips; Amcon Laboratories, Inc) were used to assess ocular surface health and scored as described in Supplemental Digital Content 1 (see Appendix 1, <http://links.lww.com/ICO/A873>).<sup>20</sup> Intraocular pressure was measured by applanation tonometry (Tonopen XL; Medtronic Solan, Jacksonville, FL) after applying 0.5% proparacaine (Alcon Inc, Fort Worth, TX). Ultrasound pachymetry (Pachette 3; DGH Technology, Inc, Exton, PA) was performed as previously described.<sup>23</sup>

### **Fourier-domain OCT and IVCM**

Fourier-domain OCT (FD-OCT) (RTVue 100, software version 6.1; Optovue Inc, Fremont, CA) and IVCM (ConfoScan 4; Nidek Technologies, Gamagori, Japan) of the central cornea were performed using the previously described methods at 2 separate sessions.<sup>23</sup> The tear meniscus was assessed using FD-OCT before sedation as previously described,<sup>24</sup> and then the dogs were intravenously sedated ( < 6 years old: dexmedetomidine 2.5 µg/kg, buprenorphine: 0.01 mg/kg; >6 years old: acepromazine 0.01 mg/kg, buprenorphine 0.01 mg/kg) for FD-OCT and IVCM of the central cornea.<sup>25</sup> Keratocytes in the anterior and posterior stroma were counted as previously described.<sup>23</sup>

## Conjunctival Biopsy and Histologic Analysis

A single conjunctival biopsy was fixed and stained with hematoxylin and eosin and scored by a single masked investigator (G.C.S.) using an established histologic scoring system.<sup>26,27</sup> Additional slides were stained with periodic acid–Schiff stain to enumerate goblet cells. Goblet cell density (GCD) was determined by counting the goblet cells per 50 consecutive epithelial cells by a single masked investigator (G.C.S.).<sup>27</sup>

## Owner Survey

A survey was collected from each client who had a dog enrolled in the study (see Appendix 2, Supplemental Digital Content 2, <http://links.lww.com/ICO/A874>). This survey was reviewed by the UC Davis Institutional Review Board and deemed exempt (IRB ID: 993,512–1). A semiquantitative scale (0–10; with 0 being no signs, 1 being very mild, and 10 being very severe) was used to evaluate disease severity at these different time points, before and during treatment.

## Statistical Analysis

Values for each animal were determined by averaging the values of each eye. Power analyses were used to estimate the sample size using the primary end point for our hypothesis, an estimate of dryness, the STT-I. Using this, it was established that for an  $\alpha$  of 0.05 and a  $\beta$  of (1–0.993), assuming mean differences of 5 mm/min with a SD of 2 mm/min predicted a sample size of 6 per group. All statistics were expressed as median with ranges, and the Mann–Whitney rank sum test was used to compare all variables except sex distribution. A Fisher exact test was used to compare sex distribution between groups.

## RESULTS

Eleven eyes from 6 WHWTs affected with ADDE (4 spayed females, 2 castrated males) and 25 eyes from 13 WHWTs unaffected with ADDE (4 spayed females, 3 intact females, 3 castrated males, 3 intact males) were included in the study; sex distribution did not significantly differ between groups (Fisher exact test,  $P = 1.000$ ). The left eye from an affected WHWT and the right eye from an unaffected WHWT were excluded from the study because of the presence of ulcerative keratitis. The mean age of ADDE-affected and ADDE-unaffected dogs did not significantly differ at  $9.3 \pm 2.1$  and  $8.8 \pm 3.5$  years, respectively ( $P = 0.78$ ); mean body weight also did not significantly differ at  $8.6 \pm 0.9$  and  $9.1 \pm 1.6$  kg, respectively ( $P = 0.42$ ). Among the affected WHWTs, there was a range of clinical signs that included thick tenacious ocular discharge, conjunctival hyperemia, corneal fibrosis, corneal neovascularization, and corneal pigmentation (Fig. 1). Median clinical scores using the SPOTS system were greater for conjunctival, corneal, and total disease scores in ADDE-affected WHWTs when compared with the control animals (Fig. 2;  $P < 0.0001$ ).<sup>20</sup> In addition, ADDE-affected animals had significantly higher median Rose bengal and lissamine green staining scores (Fig. 2;  $P = 0.04$  and  $P = 0.02$ , respectively).

ADDE-affected WHWT dogs had significantly reduced aqueous tear production, measured with both STT and PRTT, when compared with unaffected WHWT dogs (Table 1, Fig. 3;  $P < 0.0001$  and  $P = 0.0004$ , respectively). The ADDE-affected animals with the lowest

aqueous tear production tended to have higher clinical scores as previously described. Tear film stability was impaired with a significantly shorter TFBUT in ADDE-affected WHWTs than the controls (Table 1, Fig. 3;  $P < 0.0001$ ). The area under the curve meibometry measurements were significantly greater for ADDE-affected animals when compared with the controls (Table 1, Fig. 3;  $P = 0.03$ ), whereas peak meibometry measurements approached significance with ADDE-affected WHWTs having a higher value (Table 1,  $P = 0.06$ ). In addition, there was a trend toward decreased corneal sensation (corneal touch threshold values) of ADDE-affected WHWTs compared with control dogs (Table 1,  $P = 0.07$ ).

There were no statistically significant differences detected in corneal thickness with ultrasound pachymetry and no differences in the thickness of individual corneal layers between ADDE-affected and ADDE-unaffected WHWT dogs determined using FD-OCT (Table 2). FD-OCT imaging demonstrated corneal pathologies that were secondary to ADDE. One severely affected dog with ADDE had an irregular corneal surface contour, dense accumulation of corneal pigmentation visible as a hyperreflective band in the corneal epithelium with subsequent shadowing of the underlying stroma and Descemet/endothelial complex (Fig. 4A). The peripheral cornea of a moderately affected dog with ADDE lacked pigmentary changes; however, anterior stromal corneal vessels were observed, which were absent in unaffected animals (Fig. 4B). FD-OCT documented a reduced tear meniscus height with the tear content of the meniscus having a hyperreflective character consistent with dense mucous, leukocytes, and cellular debris (Fig. 4C). Using IVCM, there were no statistical differences in median cell densities in the anterior and posterior stroma, as well as the corneal endothelium when comparing ADDE-affected dogs with the controls (Table 2). Multifocal areas of granular hyperreflectivity were detected in the corneal epithelium and anterior stroma with IVCM in an ADDE-affected dog, corresponding to areas of dense corneal pigmentation (Fig. 5).

Assessment of conjunctival biopsies documented increased inflammation in ADDE-affected WHWTs. The median histologic conjunctivitis score was significantly increased between ADDE-affected WHWTs (median: 2, range: 1–3) compared with the controls (median: 0, range: 0–1;  $P < 0.001$ ). Mean GCD was not significantly different between ADDE-affected and unaffected dogs ( $P = 0.55$ ); GCD could not be determined in 2 unaffected dogs because of artifactual changes to the tissue during procurement.

Owners of all dogs (19/19) included in this study completed the survey. None of the dogs enrolled had a reported history of conditions or treatments associated with predisposing to the development of ADDE in dogs (hyperadrenocorticism, distemper virus infection, hypothyroidism, diabetes mellitus, or systemic immune-mediated disease). One of the ADDE-affected dogs had flea allergies that were controlled with topical monthly preventative, no other allergies were reported in any other dogs. In addition to the diagnosis of ADDE, 1 ADDE-affected dog was diagnosed with a previous descemetocele and another with previous conjunctivitis. The median (range) age of onset of clinical signs of ADDE was 5 (3–11) years of age ( $n = 5$ ) while one owner was uncertain. The median (range) reported severity of ADDE at the initiation of treatment and on their most effective medical regiment was 8 (6–10) and 7.5 (3–10), respectively. Owners reported using a combination of topical medications to treat ADDE. Owners assessed tacrolimus ( $n = 4$ ), tear replacement drops ( $n =$

2), cyclosporine (n = 1), neomycin-polymyxin-dexamethasone (n = 1), and gentamicin (n = 1) to be the most effective therapies. No affected dogs had undergone parotid duct transposition surgery for ADDE.

## DISCUSSION

In the WHWT, and most other cases of DED in dogs, aqueous deficiency is the presumed underlying pathogenesis of ADDE due to an immune-mediated attack on the lacrimal gland, analogous to the ADDE disease component seen in patients with Sjögren syndrome.<sup>9,10</sup> Indeed, our results confirmed that WHWTs affected by ADDE had significantly reduced aqueous tear production (lower STT and PRTT values). The magnitude of this reduction was related to the severity of clinical signs in the ADDE-affected animals because patients with the lowest tear values had the highest clinical and histologic disease severity scores. Surprisingly, the TFBUT was shortened in ADDE-affected WHWTs when compared with the controls because this change is typically associated with EDDE, and not ADDE, in humans.<sup>15</sup> However, 1 report has identified a statistically significant reduction in TFBUT in human patients with non-Sjögren syndrome ADDE, patients with meibomian gland dysfunction, and patients with combined non-Sjögren syndrome ADDE and meibomian gland dysfunction when compared with normal individuals.<sup>28</sup> Because ADDE-affected dogs are often diagnosed later in the disease course, we suspect that chronic inflammation at the ocular surface has led to damage of the transmembrane-bound mucins extending from microvilli or microplacae to stabilize the tear film.<sup>29,30</sup> We have previously demonstrated the significance of these biochemical (mucin) and biophysical (microvilli/microplacae) attributes to corneal epithelial cell wettability and hysteresis, properties directly related to tear film stability.<sup>31,32</sup> The diagnostic end points measured in this study, including TFBUT, are likely affected by these pathophysiologic alterations occurring with chronic ADDE in the WHWT and suggest that more subtle changes in ocular surface physiology may be occurring at earlier time points in the disease process. Therefore, a more thorough understanding of these ocular surface alterations would have direct implications on the development of therapeutics for ADDE that maintain these biochemical and biophysical determinants of tear film stability.

Tear osmolarity testing has high sensitivity and specificity, as well as positive predictive value, in the diagnosis of DED in humans, with higher osmolarity readings being consistent with DED.<sup>33</sup> Increased tear osmolarity triggers corneal epithelial cell damage and activation of inflammation at the ocular surface. Although identification of increased tear osmolarity has been beneficial in diagnosing and grading DED in humans, our current study and a previous investigation have demonstrated a trend toward reduced tear osmolarity.<sup>21</sup> However, there are multiple factors that complicate this assessment in dogs including the stage of disease when the test was performed, previous use of topical medications, technical difficulty with generating reproducible results with low tear volumes, and small sample size. To more accurately assess the utility of tear osmolarity in the diagnosis of ADDE in dogs, it will require a larger sample size of dogs with early examinable clinical signs of ADDE that are naive to treatment.



Despite the seemingly straight-forward diagnosis of ADDE in dogs with evidence of an aqueous tear deficiency combined with inflammation in the cornea and conjunctiva, it can be challenging to identify these patients at an earlier stage. An early diagnosis of ADDE would enable therapy to be initiated and possibly limit the inflammatory attack on the lacrimal gland, minimizing ocular surface consequences. In physician-based ophthalmic practice, there is a strong drive to use new imaging modalities to evaluate the structure and dynamic properties of the tear film, including the use of noninvasive tear film breakup time, OCT, meibomian gland imaging, IVCN, lipid layer assessment with interferometry, and thermography.<sup>34</sup> Measurement of the tear meniscus height (TMH) using OCT has a demonstrated utility in identifying human patients with DED, particularly in patients with aqueous tear deficiency.<sup>35</sup> In addition, three-dimensional imaging that combines tear meniscus height, tear meniscus area, and tear meniscus volume has improved correlation between imaging and STT.<sup>36–38</sup> Our study demonstrates the ability of anterior segment OCT to capture the tear meniscus with the potential to evaluate the efficacy of therapeutics in canine patients with ADDE.<sup>39</sup>

Overall, this study represents the most comprehensive assessment of the clinical findings, tear film diagnostic end points, and advanced imaging parameters of the ocular surface in dogs with ADDE. Because of some of the etiopathologic, clinical, and diagnostic similarities between ADDE-affected WHWTs and humans with Sjögrens syndrome (ocular disease), we speculate that WHWT dogs with ADDE could serve as a naturally occurring model for the human condition. We are currently performing a genome-wide analysis comparing controls with ADDE-affected WHWTs to identify the genetic cause(s) of their condition. Further investigations into ADDE-affected WHWT dogs are warranted to explore 1) the genetic causes of disease in this purebred population of dogs, 2) the predictive value of the model in the context of developing novel therapeutics, and 3) the underlying pathophysiologic mechanisms in a species that occupies the same environment in which we live.<sup>40</sup>

## Supplementary Material

Refer to Web version on PubMed Central for supplementary material.

## Acknowledgments

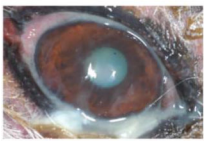
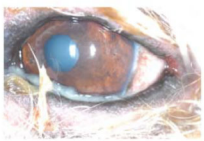


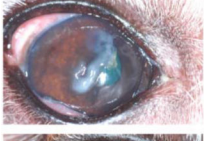


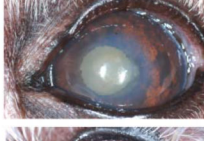
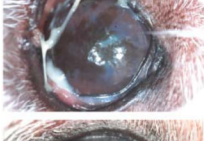
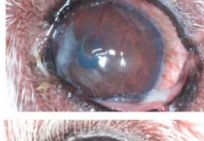


Supported by the National Institutes of Health K08EY028199 (B. C. Leonard), K08EY021142 (SMT), and R01EY016134 (C. J. Murphy), the National Eye Institute core grant P30EY12576, American Kennel Club Grant #2105 (C. J. Murphy) and matching funds from the Center for Comparative Animal Health, University of California, Davis (C. J. Murphy), and start-up funds from the School of Veterinary Medicine, University of California, Davis (S. M. Thomasy).

## REFERENCES

1. Nelson JD, Craig JP, Akpek EK, et al. TFOS DEWS II introduction. *Ocul Surf* 2017;15:269–275. [PubMed: 28736334]
2. Yu J, Asche CV, Fairchild CJ. The economic burden of dry eye disease in the United States: a decision tree analysis. *Cornea*. 2011;30:379–387. [PubMed: 21045640]
3. Craig JP, Nichols KK, Akpek EK, et al. TFOS DEWS II definition and classification report. *Ocul Surf*. 2017;15:276–283. [PubMed: 28736335]

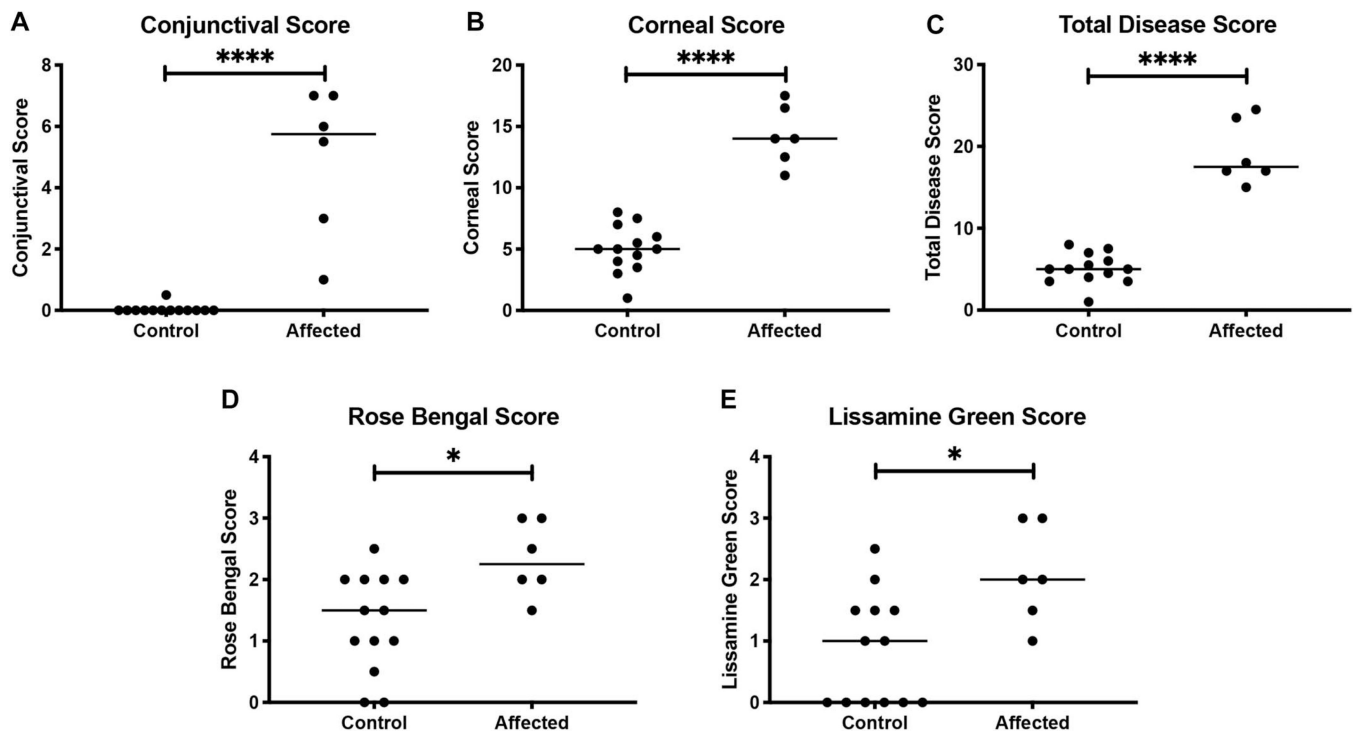
4. Holland EJ, Luchs J, Karpecki PM, et al. Lifitegrast for the treatment of dry eye disease: results of a phase III, randomized, double-masked, placebo-controlled trial (OPUS-3). *Ophthalmology*. 2017;124:53–60. [PubMed: 28079022]
5. Donnenfeld E, Pflugfelder SC. Topical ophthalmic cyclosporine: pharmacology and clinical uses. *Surv Ophthalmol*. 2009;54:321–338. [PubMed: 19422961]
6. Murphy CJ, Bentley E, Miller PE, et al. The pharmacologic assessment of a novel lymphocyte function-associated antigen-1 antagonist (SAR 1118) for the treatment of keratoconjunctivitis sicca in dogs. *Invest Ophthalmol Vis Sci*. 2011;52:3174–3180. [PubMed: 21330663]
7. Kaswan RL, Salisbury MA, Ward DA. Spontaneous canine keratoconjunctivitis sicca. A useful model for human keratoconjunctivitis sicca: treatment with cyclosporine eye drops. *Arch Ophthalmol*. 1989;107:1210–1216. [PubMed: 2757551]
8. Pflugfelder SC, de Paiva CS. The pathophysiology of dry eye disease: what we know and future directions for research. *Ophthalmology*. 2017; 124:S4–S13. [PubMed: 29055361]
9. Featherstone HJ, Heinrich CL. Ophthalmic examination and diagnostics, Part 1: the eye examination and diagnostic procedures In: Gelatt KN, Gilger BC, Kern TJ, eds. *Veterinary Ophthalmology*. Ames, IA: John Wiley & Sons; 2013:578–583.
10. Kaswan RL, Martin CL, Chapman WL Jr. Keratoconjunctivitis sicca: histopathologic study of nictitating membrane and lacrimal glands from 28 dogs. *Am J Vet Res*. 1984;45:112–118. [PubMed: 6703444]
11. Quimby FW, Schwartz RS, Poskitt T, et al. A disorder of dogs resembling Sjögren's syndrome. *Clin Immunol Immunopathol*. 1979;12:471–476. [PubMed: 455794]
12. Kaswan RL, Salisbury MA. A new perspective on canine keratoconjunctivitis sicca. Treatment with ophthalmic cyclosporine. *Vet Clin North Am Small Anim Pract*. 1990;20:583–613. [PubMed: 2194349]
13. Sanchez RF, Innocent G, Mould J, et al. Canine keratoconjunctivitis sicca: disease trends in a review of 229 cases. *J Small Anim Pract*. 2007; 48:211–217. [PubMed: 17381766]
14. Barnett KC, Sansom J. Dry eye in the dog and its treatment. *Trans Ophthalmol Soc U K*. 1985;104(pt 4):462–466. [PubMed: 3862276]
15. Wolffsohn JS, Arita R, Chalmers R, et al. TFOS DEWS II diagnostic methodology report. *Ocul Surf*. 2017;15:539–574. [PubMed: 28736342]
16. Gemensky-Metzler AJ, Sheahan JE, Rajala-Schultz PJ, et al. Retrospective study of the prevalence of keratoconjunctivitis sicca in diabetic and nondiabetic dogs after phacoemulsification. *Vet Ophthalmol*. 2015;18: 472–480. [PubMed: 25429857]
17. Williams DL, Pierce V, Mellor P, et al. Reduced tear production in three canine endocrinopathies. *J Small Anim Pract*. 2007;48:252–256. [PubMed: 17425694]
18. Sutton DJ, Roach NJ. Keratoconjunctivitis sicca associated with potentiated sulphonamides. *Vet Rec*. 1988;122:262.
19. Klaus G, Giuliano EA, Moore CP, et al. Keratoconjunctivitis sicca associated with administration of etodolac in dogs: 211 cases (1992–2002). *J Am Vet Med Assoc*. 2007;230:541–547. [PubMed: 17302553]
20. Eaton JS, Miller PE, Bentley E, et al. The SPOTS system: an ocular scoring system optimized for use in modern preclinical drug development and toxicology. *J Ocul Pharmacol Ther*. 2017;33:718–734. [PubMed: 29239680]
21. Sebbag L, Kass PH, Maggs DJ. Reference values, intertest correlations, and test-retest repeatability of selected tear film tests in healthy cats. *J Am Vet Med Assoc*. 2015;246:426–435. [PubMed: 25632817]
22. Hawkins EC, Murphy CJ. Inconsistencies in the absorptive capacities of Schirmer tear test strips. *J Am Vet Med Assoc*. 1986;188:511–513. [PubMed: 3957758]
23. Thomasy SM, Cortes DE, Hoehn AL, et al. In vivo imaging of corneal endothelial dystrophy in Boston terriers: a spontaneous, canine model for fuchs' endothelial corneal dystrophy. *Invest Ophthalmol Vis Sci*. 2016; 57:OCT495–503. [PubMed: 27454658]
24. Wang J, Cui L, Shen M, et al. Ultra-high resolution optical coherence tomography for monitoring tear meniscus volume in dry eye after topical cyclosporine treatment. *Clin Ophthalmol*. 2012;6:933–938. [PubMed: 22791975]

25. Strom AR, Cortés DE, Rasmussen CA, et al. In vivo evaluation of the cornea and conjunctiva of the normal laboratory beagle using time- and Fourier-domain optical coherence tomography and ultrasound pachymetry. *Vet Ophthalmol.* 2016;19:50–56. [PubMed: 25676065]
26. Sebbag L, Reilly CM, Eid R, et al. Goblet cell density and distribution in cats with clinically and histologically normal conjunctiva. *Vet Ophthalmol.* 2016;19(suppl 1):38–43.
27. Lim CC, Reilly CM, Thomasy SM, et al. Effects of feline herpesvirus type 1 on tear film break-up time, Schirmer tear test results, and conjunctival goblet cell density in experimentally infected cats. *Am J Vet Res.* 2009;70:394–403. [PubMed: 19254153]
28. Arita R, Morishige N, Koh S, et al. Increased tear fluid production as a compensatory response to meibomian gland loss: a multicenter cross-sectional study. *Ophthalmology.* 2015;122:925–933. [PubMed: 25626757]
29. Argüeso P, Gipson IK. Epithelial mucins of the ocular surface: structure, biosynthesis and function. *Exp Eye Res.* 2001;73:281–289. [PubMed: 11520103]
30. Willcox MDP, Argüeso P, Georgiev GA, et al. TFOS DEWS II tear film report. *Ocul Surf.* 2017;15:366–403. [PubMed: 28736338]
31. Yanez-Soto B, Leonard BC, Raghunathan VK, et al. Effect of stratification on surface properties of corneal epithelial cells. *Invest Ophthalmol Vis Sci.* 2015;56:8340–8348. [PubMed: 26747762]
32. Leonard BC, Yañez-Soto B, Raghunathan VK, et al. Species variation and spatial differences in mucin expression from corneal epithelial cells. *Exp Eye Res.* 2016;152:43–48. [PubMed: 27614208]
33. Potvin R, Makari S, Rapuano CJ. Tear film osmolarity and dry eye disease: a review of the literature. *Clin Ophthalmol.* 2015;9:2039–2047. [PubMed: 26586933]
34. Chan TCY, Wan KH, Shih KC, et al. Advances in dry eye imaging: the present and beyond. *Br J Ophthalmol.* 2018;102:295–301. [PubMed: 28982950]
35. Ibrahim OM, Dogru M, Takano Y, et al. Application of visante optical coherence tomography tear meniscus height measurement in the diagnosis of dry eye disease. *Ophthalmology.* 2010;117:1923–1929. [PubMed: 20605216]
36. Fukuda R, Usui T, Miyai T, et al. Tear meniscus evaluation by anterior segment swept-source optical coherence tomography. *Am J Ophthalmol.* 2013;155:620–624, 624 e621–622. [PubMed: 23317654]
37. Akiyama R, Usui T, Yamagami S. Diagnosis of dry eye by tear meniscus measurements using anterior segment swept source optical coherence tomography. *Cornea.* 2015;34(suppl 11):S115–S120. [PubMed: 26448168]
38. Akiyama-Fukuda R, Usui T, Yoshida T, et al. Evaluation of tear meniscus dynamics using anterior segment swept-source optical coherence tomography after topical solution instillation for dry eye. *Cornea.* 2016;35:654–658. [PubMed: 26989953]
39. Napoli PE, Satta GM, Coronella F, et al. Spectral-domain optical coherence tomography study on dynamic changes of human tears after instillation of artificial tears. *Invest Ophthalmol Vis Sci.* 2014;55: 4533–4540. [PubMed: 24985473]
40. Kol A, Arzi B, Athanasiou KA, et al. Companion animals: translational scientist’s new best friends. *Sci Transl Med.* 2015;7:308ps21.

Clinical Images		PRTT OD   OS	STT-I OD   OS	TFBUT OD   OS
OD	OS			
		2   8	9   11	3.6   5.3
		8   ND	3   ND	3.7   ND
		16   8	3   8	2.3   2.3
		3   5	3   3	3.1   3.8
		2   8	0   0	5.8   2.6
		3   4	2   2	1.2   1.4

**FIGURE 1.**

ADDE-affected animals have a spectrum of clinical signs that correlate with reduced tear film diagnostic results. Representative clinical images of the left and right eyes of ADDE-affected WHWTs with variable clinical signs characterized by mucoid discharge, conjunctival hyperemia and chemosis, corneal fibrosis, neovascularization, and melanosis dependent on the severity of disease. PRTT (mm/15 s), STT-I (mm/60 s), and TFBUT (s) values recorded for each ADDE-affected WHWT. ND indicates no data recorded because of the presence of a corneal ulcer in that eye.

**FIGURE 2.**

ADDE-affected WHWT dogs ( $n = 6$ ) have higher median conjunctival, corneal, total disease, and vital dye staining scores when compared with unaffected WHWT dogs ( $n = 13$ ). A, Conjunctival disease scores determined by the presence of conjunctival congestion, chemosis, and discharge. B, Corneal disease scores determined by the presence of corneal opacity severity, the surface area affected by opacity, corneal vascularization, and depth. C, Total disease score represents the addition of conjunctival and corneal disease scores. (D + E) Rose bengal and lissamine green staining scores determined the number of positive staining foci or the percentage of the corneal/conjunctival surface area that retains vital stain. Each dot represents the mean value of both eyes for a given individual, and the horizontal line indicates the median value of the group; \* $P < 0.05$ , \*\*\*\* $P < 0.0001$ .

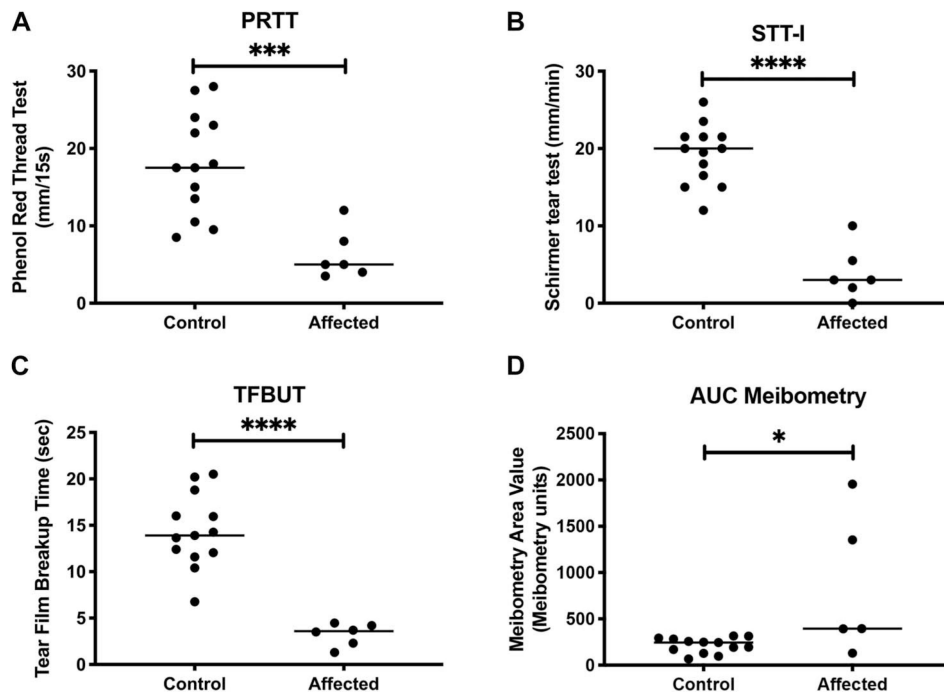


**FIGURE 3.**

ADDE-affected WHWT dogs ( $n = 6$ ) have lower aqueous and mucin tear parameters yet increased lipid tear content when compared with unaffected WHWT dogs ( $n = 13$ ). Aqueous tear deficiency in ADDE-affected dogs was demonstrated by a reduced PRTT (A) and STT-I (B). A mucin tear deficiency in ADDE-affected dogs was demonstrated by a reduced TFBUT (C). An increased lipid content in the tear film was detected using area under the curve meibometry (D). Each dot represents the mean value of both eyes for a given individual, and the horizontal line indicates the median value of the group; \* $P < 0.05$ , \*\*\* $P < 0.0005$ , \*\*\*\* $P < 0.0001$ .

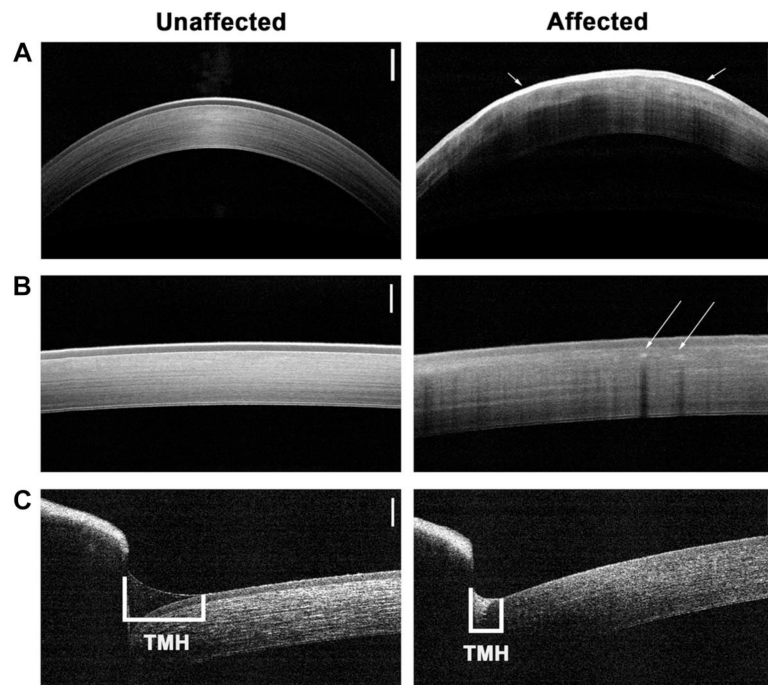


**FIGURE 4.**

Advanced imaging with FD-OCT identified both compositional and structural changes to the cornea and tear meniscus differences in ADDE-affected WHWTs, but not present in unaffected controls. A, Long-axis lens view of the central cornea of an unaffected and ADDE-affected WHWT. The ADDE-affected WHWT dog has a hyperreflective corneal epithelium (short arrows) consistent with pigmentation of the epithelium and distal shadowing likely an artifact of the pigmentation signal. Size bar equivalent to 250  $\mu\text{m}$ . B, Short-axis lens view of the peripheral cornea of an unaffected and ADDE-affected WHWT. The ADDE-affected WHWT dog has evidence of anterior stromal neovascularization (long arrows) with distal shadowing artifact. Size bar equivalent to 250  $\mu\text{m}$ . C, Short axis lens view of the inferior tear meniscus of an unaffected and ADD-Eaffected WHWT. The tear meniscus height (bracket) in the unaffected WHWT is longer than the ADDE-affected dog. In addition, there is increased hyperreflectivity of the tear meniscus in the ADDE-affected WHWT, likely because because of increased cellularity in the tear film. Size bar equivalent to 250  $\mu\text{m}$ .

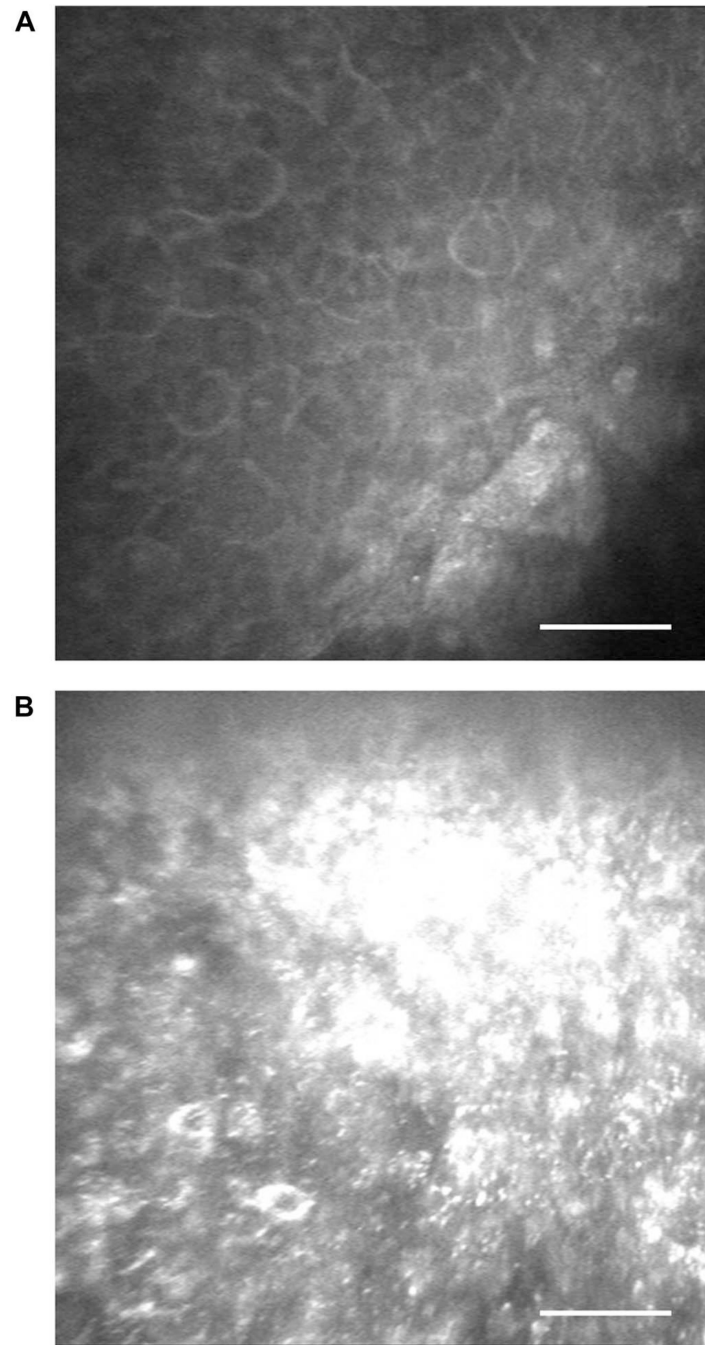


**FIGURE 5.** ICVM documented areas of corneal epithelial lesions from a single ADDE-affected WHWT dog. A, Normal corneal epithelial cells with distinct intercellular borders and clearly defined nuclei, with a focal area of corneal epithelial pigmentation in the bottom right quadrant. B, Diffuse dense pigmentation of the corneal epithelial cells. Size bar equivalent to 50 μm.



**TABLE 1.**

## Diagnostic Assessment of Tear Film and Ocular Surface Parameters

	Control (Range; n)	Affected (Range; n)	<i>P</i>
Tear Film Parameter			
Tear osmolarity (mOsm/L)	339 (316–369; 13)	346 (344–369; 3)	0.2
Quantitative tear assessment			
PRTT (mm/15 s)	17.5 (8.5–28.0; 13)	5.0 (3.5–12.0; 6)	0.0004
STT (mm/min)	20 (12–26; 13)	3 (0–10; 6)	<0.0001
Qualitative tear assessment			
TFBUT (s)	13.9 (6.8–20.5; 13)	3.6 (1.3–4.5; 6)	<0.0001
Meibometry			
Area under curve (MU)	245 (68–315; 13)	394 (130–1954; 5)	0.03
Peak measurement (MU)	89 (31–181; 13)	201 (77–437; 5)	0.06
Ocular surface parameter			
Corneal touch threshold (g/mm <sup>2</sup> )	1.4 (0.6–2.3; 13)	2.2 (1.2–10.3; 6)	0.07

**TABLE 2.**

Advanced Imaging Assessment of Central Corneal Thickness Assessed by Ultrasound Pachymetry, Individual Corneal Layer Thickness and Total Thickness Assessed by FD-OCT, and Cellular Density Assessed by IVCM

Median thickness measurement ( $\mu\text{m}$ )	Control (Range; n)	Affected (Range; n)	<i>P</i>
Pachymetry: central	611 (547–707; 13)	650 (548–903; 6)	0.7
Epithelium	53 (52–71; 3)	64 (56–72; 2)	0.4
Stroma	501 (494–557; 3)	544 (473–614; 2)	>0.9999
Endothelium/Descemet	24 (22–25; 3)	24 (24–25; 2)	0.8
Total thickness	572 (551–620; 3)	615 (533–697; 2)	>0.9999
Median cellular density (cells/ $\text{mm}^2$ )	Control (Range; n)	Affected (Range; n)	<i>P</i>
Anterior stromal density	634 (540–647; 3)	669 (638–700; 2)	0.8
Posterior stromal density	525 (500–545; 3)	582 (562–602; 2)	0.2
Endothelial cell density	1878 (1693–2059; 3)	2061 (1823–2299; 2)	0.8